Polymer memory device based on conjugated polymer and gold nanoparticles

Ankita Prakash and Jianyong Ouyang
Department of Materials Science and Engineering, University of California, Los Angeles, California 90095

Jen-Lien Lin
Union Chemical Laboratories, Industry Technology Research Institute, Hsinchu 300, Taiwan, Republic of China

Yang Yang[a)]
Department of Materials Science and Engineering, University of California, Los Angeles, California 90095

(Received 6 February 2006; accepted 20 June 2006; published online 8 September 2006)

Electrical bistability is demonstrated in a polymer memory device with an active layer consisting of conjugated poly(3-hexylthiophene) and gold nanoparticles capped with 1-dodecanethiol sandwiched between two metal electrodes. The device was fabricated through a simple solution processing technique and exhibited a remarkable electrical bistable behavior. Above a threshold voltage the pristine device, which was in a low conductivity state, exhibited an increase in conductivity by more than three orders of magnitude. The device could be returned to the low conductivity state by applying a voltage in the reverse direction. The electronic transition is attributed to an electric-field-induced charge transfer between the two components in the system. The conduction mechanism changed from a charge-injection-controlled current in the low conductivity state to a charge-transport-controlled current in the high conductivity state. In the high conductivity state the conduction was dominated by a field-enhanced thermal excitation of trapped charges at room temperature, while it is dominated by charge tunneling at low temperatures. The device exhibited excellent stability in both the conductivity states and could be cycled between the two states for numerous times. The device exhibits tremendous potential for its application as fast, stable, low-cost, high storage density nonvolatile electronic memory. © *2006 American Institute of Physics*. [DOI: 10.1063/1.2337252]

I. INTRODUCTION

During the past few years tremendous work has been done in the field of conducting polymers and polymer based electronic devices. This class of materials provides a variety of interesting properties, which facilitate the realization of electronic devices with advantages over the existing inorganic semiconductor devices. These include low fabrication cost- high mechanical flexibility. Devices such as light emitting diodes (LEDs),[1,2] field effect transistors,[3,4] and solar cells,[5] have showed a great potential towards future technologies. Recently, memory devices using organic or polymer materials were demonstrated,[6–11] which opened a direction in organic/polymer electronics. Compared to the inorganic memory technology, these organic/polymer memory devices have many advantages, including high flexibility, high response speed, and high device density due to the possibility of stacking these devices. Moreover, polymer memory has the advantage of simple fabrication process and good controllability of materials. Several types of polymer memory devices have been reported. Ouyang *et al.* reported a simple field programmable memory using a blend of conjugated small molecule and gold nanoparticles in a polymer matrix and proposed that the electronic transition is due to an electric-field-induced charge transfer between gold nanoparticle and the conjugated organic moleucle.[9] A single component memory device was reported by Tseng *et al.* based on nanofibers of polyaniline decorated with gold nanoparticles.[10] Chu *et al.* reported an all-organic (metal-free) memory based on an electron donor-acceptor composite organic system.[11] More recently, Beinhoff *et al.* demonstrated the synthesis of polymers for application to stable memory devices.[12]

In the above polymer memory devices based on polymer and nanoparticle,[9,10] inert polymers, such as polystyrene and polyvinyl alcohol, were used as matrix. A direct usage of the polymer as both matrix and active component would simplify the device. It will be also helpful to control the materials and understand the relation between the materials structure and device performance. Therefore, we describe the fabrication and operation of a nonvolatile memory device based on a conjugated polymer and nanoparticle composite, where the conjugated polymer serves both as matrix and active component of the device. It was fabricated by a simple solution processing technique and exhibited a very high stability and excellent performance. The device exhibited a high stability in both the conductivity states and showed a switching behavior even at very low temperatures. Moreover, the device showed excellent performance even after a larger number of read-write-erase cycles.

[a)]Electronic mail: yangy@ucla.edu

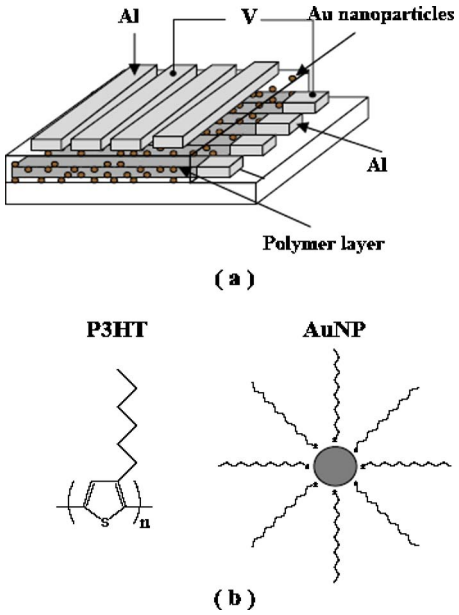

FIG. 1. (Color online) (a) Device structure and (b) chemical structures of P3HT and the Au NP.

II. EXPERIMENT

Poly(3-hexylthiophene) (P3HT) was purchased from Rieke Metals, Inc. The gold nanoparticles (Au NPs) were prepared by the two-phase arrested growth method.[22] They had a size distribution of 1.6–4.4 nm and an average particle size of 2.8 nm. The device was fabricated by the following process. The first step involved preparation of the substrate. Glass substrates were cleaned thoroughly by a series of ultrasonications in different solvents such as detergent, deionized water, acetone, and isopropyl alcohol. After the substrates were dried for 3–4 h and subsequently treated with UV ozone, the bottom Al electrode was deposited by thermal evaporation in a vacuum of $\sim 10^{-6}$ Torr. Then, the bottom electrode was treated with UV ozone, and an active polymer layer of 40 nm was formed by spin coating a 1,2-dichlorobenzene solution of P3HT and Au NPs. The polymer solution was prepared by mixing P3HT solution and Au NP solution. Polymer films were obtained by spin-coating solutions of different P3HT and Au NP concentrations on glass substrates. The optimum solution is of 1.2 wt % P3HT and 0.24 wt % Au NPs. Finally, the top Al electrode was deposited. Both the electrodes have a thickness of 70 nm and a linewidth of 0.2 mm. The device had an area of 0.2×0.2 mm^2. Al/AuNPs+P3HT/Al is used to represent this device.

Current-voltage (*I-V*) curves, write-read-erase cycles, and stress tests of the device were tested in a vacuum of 10^{-5} Torr using an HP 4155B semiconductor parameter analyzer and a Janis temperature-variable probe station. The *I-V* curves at low temperature were tested using liquid nitrogen as coolant.

III. RESULTS AND DISCUSSION

The device has a simple structure with a polymer layer sandwiched between two aluminum electrodes [Fig. 1(a)].

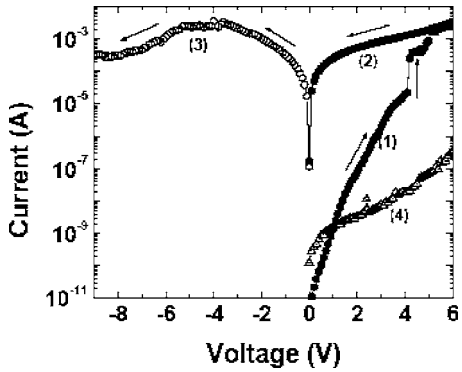

FIG. 2. Current-voltage (*I-V*) curves for the Al/Au NPs+P3HT/Al and Al/P3HT/Al devices. Curves (1), (2), and (3) represent the first, second, and third bias scans of the former device, with the arrows indicating the direction of the scans, and curve (4) is the *I-V* curve of the latter device.

The active layer consists of a P3HT film containing 1-dodecanethiol-capped gold nanoparticles. Chemical structures of both the components have been shown in Fig. 1(b). Gold nanoparticles are selected in our devices, since gold nanoparticles capped with alkanethiol, which have a good solubility in many organic solvents, have been extensively studied.[22]

The current-voltage (*I-V*) curve of the device is shown in Fig. 2. The pristine device exhibited a low current at small bias. A current jump is observed above a threshold voltage of around 3–4 V [curve (1) in Fig. 2]. In the subsequent scan the device remains in the high conductivity state (on state) [curve (2) in Fig. 2]. The current at 1 V is higher by more than four orders of magnitude than that of the pristine device. The currents through a device at 1 V in the low and high conductivity states were of the order of 10^{-9} and 10^{-4} A, respectively. After the transition to the high conductivity state, the device could be returned to the low conductivity state (off state) by applying a negative bias of −10 V. On the other hand, the device Al/P3HT/Al without Au NPs in the polymer layer did not exhibit a significant current hysteresis [curve (4) in Fig. 2].

Though the device exhibited a repeatable switching behavior between two conductivity states, the electrical behavior was not exactly the same as that in the device using gold nanoparticle and 8-hydroxyquinoline.[9] This device exhibited a higher current in the off state and a more gradual transition between the two conductivity states. These differences may be attributed to the structure of the organic and polymer materials. Conjugated P3HT has a higher highest occupied molecular orbital (HOMO) and lower lowest unoccupied molecular orbital (LUMO) than 8-hydroxyquinoline. In addition, the charge carrier mobility in a P3HT film should be higher than in a polystyrene film dispersed with 8-hydroxyquinoline.

Electrical switching between the two conductivity states of the device was able to perform thousand times. Figure 3(a) shows the current at 1 V of the device in the two conductivity states. The "on" current at 1 V was taken after applying a voltage pulse of 5 V to the device, while the "off" current at 1 V was recorded after applying a voltage pulse of −10 V to the device. The on current exhibited a little de-

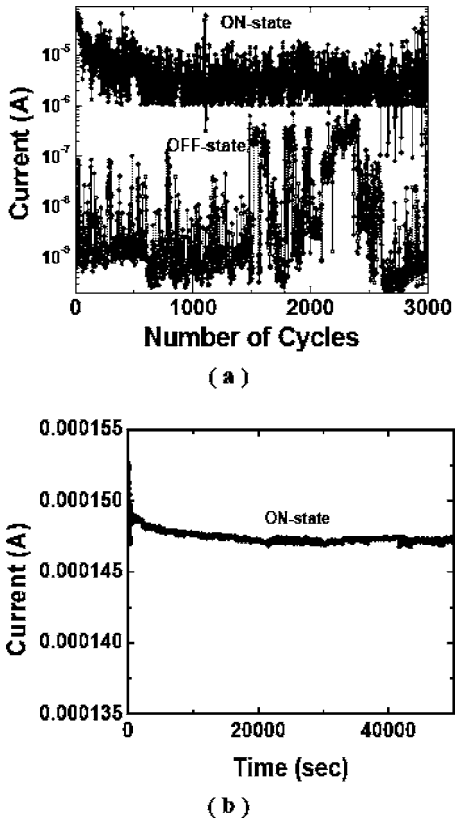

FIG. 3. (a) Currents of the Al/Au NPs+P3HT/Al device at 1 V after cycling write (apply a voltage of 5 V to the device) and erase (apply a voltage of −10 V to the device) processes. (b) Stress test for the device in the on state by applying a constant voltage of 1 V to the device.

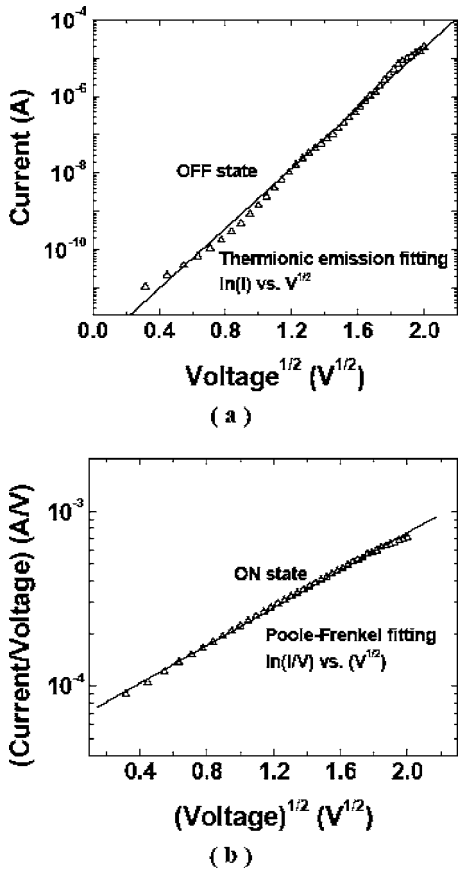

FIG. 4. *I-V* curve of the Al/P3HT+Au NPs/Al device in the (a) off state and (b) on state. The scatters are experimental data, and the straight lines are the fitting using theoretical models.

crease with the increasing cycling times at the first 100 cycles but was still higher by more than three orders of magnitude than the off current. Fluctuation of the off current appeared after 1500 cycles.

Thus, the electrical bistability of the device could be precisely controlled and detected by the application of bias and measure of current through the device. In addition to this, the device was stable in both the conductivity states. Stress tests were performed by subjecting the device to a low bias of 1 V over prolonged periods of time. When subjected to this test the device in the low conductivity state retained its conductivity and did not undergo any transition to the higher conductivity state. Similar tests were performed on the device in the high conductivity state [Fig. 3(b)]. After 13 h test, the current at 1 V did not exhibit a remarkable change. This current almost kept constant even after three days. The device demonstrated excellent retention of the high conductivity state. This stability could be further improved by the optimization of the device parameters and experimental conditions.

Further experiments were carried out to study the transition mechanism. Our experimental results indicated that the threshold voltage for transition increases with increasing thickness of the active layer and the device performance is related to the concentration of the gold nanoparticles. Thus, the electric transition may be due to the electric-field effect, and gold nanoparticles play an important role for the electrical transition.

To understand the conduction mechanism through the device, the *I-V* curves of the device in both states were analyzed in terms of theoretical models.[13] A linear relation was observed between $\log I$ and $V^{1/2}$ [Fig. 4(a)] from 0 to 3 V for the device in the off state. This suggests that the off current is probably controlled by charge injection from the Al electrode.[14] This is understandable in terms of the energy levels. The Al electrode has a work function of 4.2 eV; P3HT has a LUMO level of 3.0 V and a HOMO level of 5.1 eV.[15,16] Hence, there is an energy barrier between the Al electrode and the P3HT layer, and the charge injection through the energy barrier dominates the conduction mechanism.

The *I-V* relation changed after the electrical transition to the on state. A linear relation was observed between $\log(I/V)$ and $V^{1/2}$ [Fig. 4(b)]. This suggested that after the transition the current through the device may change to Poole-Frenkel emission, which is defined as a field-enhanced thermal emission of trapped charges[11,17,18] given by

$$I = C_0 V e^{-(q/KT)[\phi-(qV/\pi\varepsilon l)^{1/2}]}, \tag{1}$$

where I denotes the current through the device, V the bias, q the electronic charge, ϕ the potential barrier height, ε the dynamic permittivity, K the Boltzmann constant, T the temperature, and C_0 is a constant.

Low temperature measurements were carried out on the device to further study the conduction mechanism. The mea-

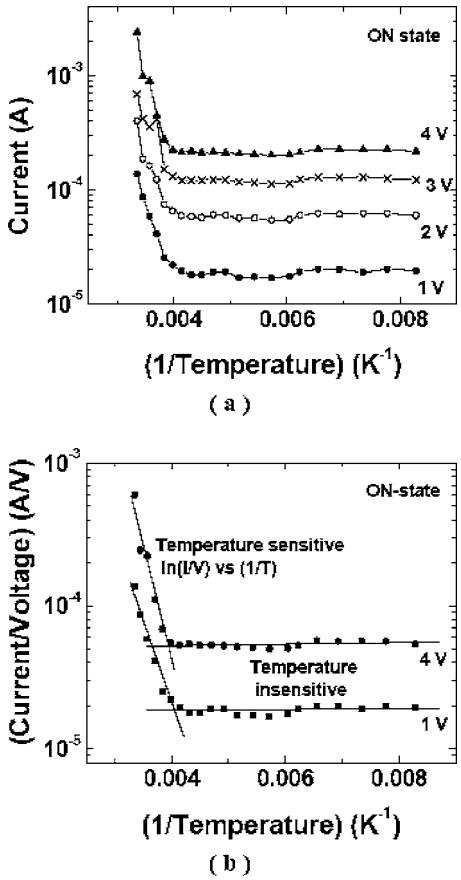

FIG. 5. (a) Temperature dependence of currents at 1, 2, 3, and 4 V for the device in the on state. (b) $\log(I/V)$ vs $1/T$ at 1 and 4 V for the device in the on state. The lines are the fitting of the experimental data using theoretical models.

surements showed two distinct regions in the $\log(I)$ vs $1/T$ plot [Fig. 5(a)]. At temperature range from room temperature to 240 K, the *I-V* characteristic showed a strong dependence on temperature. The on current decreases with lowering temperature, and there is a linear relation between $\log(I/V)$ and $(1/T)$ [Fig. 5(b)]. The activate energy is 0.13–0.14 eV. This temperature dependence of the current confirms the Poole-Frenkel emission conduction mechanism for the device in the on state.

On the other hand, the current-voltage and current-temperature relations change at a temperature below 240 K. As indicated in Fig. 5(a), the current becomes insensitive to the temperature at the temperature below 240 K. In addition, the current-voltage relation changes into a linear relation between $\ln(I/V^2)$ and $(1/V)$ (Fig. 6). These results suggest that the conduction mechanism for the device in the on state may change to Fowler-Nordheim tunneling at low temperature. The formulation for Fowler-Nordheim tunneling is[19]

$$I = C_1 V^2 e^{-4d\Phi^{3/2}(2m^*)^{1/2}/3q\eta V}, \tag{2}$$

where Φ denotes the energy barrier height, d the tunneling distance, m^* the effective mass of the charge carrier, C_1 is a constant, and other parameters are the same as in formula (1).

To further understand the role of the gold nanoparticles in the polymer film, comparative experiments were performed on devices using P3HT only (without Au NPs). The conduction mechanism for the Al/P3HT/Al device studied by analyzing the current-voltage and current-temperature relations revealed that the conduction mechanism is charge-injection-limited current at low bias and changes to space-charge-limited current at high voltage. They are similar to the conduction mechanisms of the device ITO/P3HT/Al.[20] This comparative study suggests that the trap for the Poole-Frenkel emission of the Al/P3NT+Au NPs/Al in the on state is due to the presence of the gold nanoparticles in the polymer film.

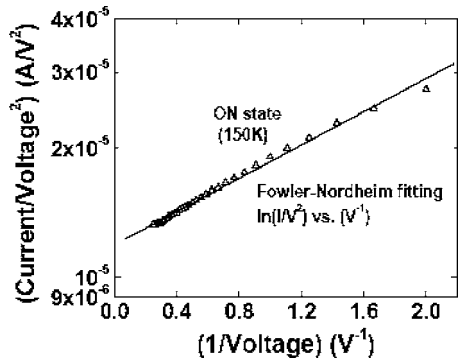

FIG. 6. *I-V* curve for the device in the on state at 150 K. The scatters are experimental data, and the straight line is the fitting of the data by Fowler-Nordheim tunneling model.

Based on the above results, we propose that the electronic transition is due to an electric-field-induced charge transfer between gold nanoparticles and P3HT. When the external electric field is high enough, electron on the HOMO of P3HT may gain enough energy and tunnel through 1-dodecanethiol into the core of gold nanoparticles (Fig. 7). Consequently, the gold nanoparticles are negatively charged while P3HT are positively charged. The negative charge on a gold nanoparticle may be stable due to the insulator

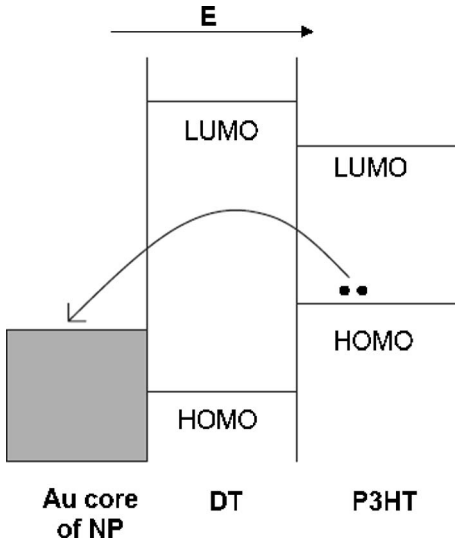

FIG. 7. Energy diagram of the core of gold nanoparticle, 1-dodecanethiol (DT), and poly(3-hexylthiophene) (P3HT). The two dots on the HOMO of P3HT represent two electrons, *E* indicates the direction of the electric field, and the arrow from the electrons on the HOMO of P3HT indicates the electron transfer from P3HT to the core of gold nanoparticle.

1-dodecanethiol shell.[21] The effect of the charge transfer on the electronic structure of P3HT is similar to the chemical oxidation of conducting polymer. It is well known that the conductivity of a conducting polymer significantly increases after chemical oxidation.[23] The returning of the device from on to off state is due to the turning back of the electron from gold nanoparticle to P3HT. This proposed mechanism is similar to that of the devices using other materials, such as gold nanoparticles and 8-hydroxyquinoline, polyaniline nanofibers decorated with gold nanoparticles, and organic donor and acceptor.[9–11]

Though the electronic transition mechanism for this device is very similar to that for the device using gold nanoparticle and 8-hydroxyquinoline, the electrical behaviors of the two devices have some differences. The conduction mechanisms are Poole-Frenkel emission and Fowler-Nordheim tunneling for the former and latter devices in the on state at room temperature, respectively. Presumably, this is due to the different charge transport through the organic or polymer materials. Charge transport through P3HT is through charge hopping among the polymer film, while charge transport through 8HQ dispersed in an inert polymer film may be through charge tunneling among the molecules. The effect of the Coulomb interaction between the negative charge on gold nanoparticle and the positive charge on P3HT chain can be observed because of a high charge mobility on the polymer film, while the effect becomes less significant because of the low charge carrier mobility among the 8-hydroxyquinoline molecules. Another difference of the electrical behavior for the two devices is the erasing voltage. The former device exhibits a much higher voltage than the turning-on voltage. The reason may be related to the stability of the charge in the polymer. After the charge transfer, hole will delocalize in the whole P3HT chains so that the whole system may become more stable after the charge transfer. This is in contrary to the device using gold nanoparticle and 8-hydroxyquinoline.

IV. CONCLUSIONS

In conclusion, a polymer bistable device using conjugated polymer and gold nanoparticles has been demonstrated. This device exhibited an electric-field-induced transition from a charge-injection-limited current to a trap-controlled current. The charge conduction for the device in the on state is mainly due to the field-enhanced thermal excitation of trapped charges at room temperature, while it changes to Fowler-Nordheim tunneling at low temperature. The device exhibits a repeatable bistable behavior and high stability in either state. These characteristics indicate the device strong potential towards its application as nonvolatile electronic memory.

ACKNOWLEDGMENTS

This research is sponsored by the Air Force Office of Scientific Research (FA9550-04-1-02) and the National Science Foundation (DMR-0305111).

[1] J. H. Burroughes, D. D. C. Bradley, A. R. Brown, R. N. Marks, K. Mackay, R. H. Friend, P. L. Burns, and A. B. Holmes, Nature (London) **347**, 539 (1990).
[2] Q. Xu, J. Huang, and Y. Yang, J. Soc. Inf. Disp. **13**, 411 (2005).
[3] C. D. Dimitrakopoulos and D. J. Mascaro, IBM J. Res. Dev. **45**, 11 (2001).
[4] L. Ma and Y. Yang, Appl. Phys. Lett. **85**, 5084 (2004).
[5] N. S. Sariciftci, L. Smilowitz, A. J. Heeger, and F. Wudl, Science **258**, 1474 (1992).
[6] L. Ma, J. Liu, and Y. Yang, Appl. Phys. Lett. **80**, 2997 (2002).
[7] J. Wu, L. P. Ma, and Y. Yang, Phys. Rev. B **69**, 115321 (2004).
[8] L. D. Bozano, B. W. Kean, V. R. Deline, J. R. Salem, and J. C. Scott, Appl. Phys. Lett. **84**, 607 (2004).
[9] J. Ouyang, C.-W. Chu, C. Szmanda, L. Ma, and Y. Yang, Nat. Mater. **3**, 918 (2004).
[10] R. J. Tseng, J. Huang, J. Ouyang, R. B. Kaner, and Y. Yang, Nano Lett. **5**, 1077 (2005).
[11] C. W. Chu, J. Ouyang, J. H. Tseng, and Y. Yang, Adv. Mater. (Weinheim, Ger.) **17**, 1440 (2005).
[12] M. Beinhoff, L. D. Bozano, J. C. Scott, and K. R. Carter, Macromolecules **38**, 4147 (2005).
[13] W. Brutting, S. Berleb, and A. G. Muckle, Org. Electron. **2**, 1 (2001).
[14] E. H. Rhoderick and R. H. Williams, *Metal-Semiconductor Contacts* (Clarendon, Oxford, 1988).
[15] D. Chirvase, Z. Chiguvare, M. Knipper, J. Parisi, V. Dyakonov, and J. C. Hummelen, Synth. Met. **1**, 10348 (2003).
[16] R. Valaski, L. M. Moreira, L. Micaroni, and I. A. Hummelgen, J. Appl. Phys. **92**, 2035 (2002).
[17] J. Frenkel, Phys. Rev. **54**, 647 (1938).
[18] S. M. Sze, *Physics of Semiconductor Devices* (Wiley Interscience, New York 1999).
[19] W. Wang, T. Lee, and M. A. Reed, Phys. Rev. B **68**, 035416 (2003).
[20] Z. Chiguvare, J. Parisi, and V. Dyakonov, J. Appl. Phys. **94**, 2440 (2003).
[21] S. Chen *et al.*, Science **280**, 2098 (1998).
[22] M. J. Hostetler *et al.*, Langmuir **14**, 17 (1998).
[23] H. Shirakawa, E. J. Louis, A. G. MacDiarmid, C. K. Chiang, and A. J. Heeger, J. Chem. Soc., Chem. Commun. 1977, 579.